IEEE Access
Multidisciplinary | Rapid Review | Open Access Journal

IEEE POWER & ENERGY SOCIETY SECTION

Received 9 July 2023, accepted 16 August 2023, date of publication 22 August 2023, date of current version 30 August 2023.

Digital Object Identifier 10.1109/ACCESS.2023.3307466

RESEARCH ARTICLE

ANFIS-Based Fault Distance Locator With Active Power Differential-Based Faulty Line Identification Algorithm for Shunt and Series Compensated Transmission Line Using WAMS

V. SREELEKHA AND A. PRINCE, (Senior Member, IEEE)
Department of Electrical Engineering, Rajiv Gandhi Institute of Technology Kottayam, APJ Abdul Kalam Technological University, Thiruvananthapuram, Kerala 695016, India

Corresponding author: V. Sreelekha (svlekha@gmail.com)

ABSTRACT In power systems, it is challenging to identify the faulty line and fault distance when compensating devices are present in the system. This work presents a fault locator using an Adaptive-Network-based Fuzzy Inference System (ANFIS) that accurately estimates the fault location on a compensated line in conjunction with an active power differential-based backup protection algorithm for faulty line identification. Both the faulty line identification algorithm and the ANFIS-based fault locator utilise the positive and negative sequence voltage and current phasors generated by the Phasor Measurement units (PMUs) placed in the system. The ANFIS-based fault locator is trained and tested using the simulated fault data obtained with a MATLAB Simulink model of a modified WSCC 9 bus system. The training data is generated by varying the fault distance in steps of 10 km. The line-to-line resistance (Rf) of 0.01 Ω, 0.1 Ω & 1 Ω, and the line-to-ground resistance (Rg) 1 Ω, 10 Ω & 100 Ω are used with different types of faults (LG, LLG, LLLG, LL& LLL) for training. Two ANFIS structures are trained for the fault distance estimation in compensated line - one for Static Synchronous Compensator (STATCOM) and the other for Static Synchronous Series Compensator (SSSC). Simulation results show the fault locator estimates the fault location accurately with a 5% tolerance in all the fault conditions simulated.

INDEX TERMS Active power differential, ANFIS, compensated line, fault location, hierarchial, STATCOM, SSSC, WAMS.

I. INTRODUCTION

To fix problems when a fault in a power transmission system arises, the location of the fault must have been identified. The power system problems with the highest likelihood of happening are transmission line faults. It is possible to locate the fault using the variation in voltage and currents at the moment the issue occurred. The impedance that the distance relays detect helps to calculate the fault distances. The location of the fault can be estimated using the mathematical models of the transmission lines. However, modelling becomes more challenging when compensating devices are involved, and fault location identification is accurate only if the behaviour of the compensating device under various operating conditions is effectively modelled.

The introduction of compensating devices in a transmission line can cause maloperation of the protection schemes and erroneous fault distance estimation. When the device is included in the fault loop, it affects the apparent impedance seen by the distance relay causing its maloperation. The type of the compensating device has also an effect on the apparent impedance seen by the relay and trip boundary.

The associate editor coordinating the review of this manuscript and approving it for publication was Sarasij Das.

A backup protection scheme based on the magnitudes and angles of positive and negative sequence voltages and currents is found more effective in the presence of series compensation [1]. Modification of line impedance seen by the existing relay [2] by estimating the voltage across the series compensation device can improve reliability. Spectral energy calculations based differential protection scheme using the Discrete Wavelet Transform (DWT) technique are proposed in [3] for lines with Static Var Compensator (SVC). Fault detection in Fixed Series Capacitor (FSC) compensated lines can be achieved using differential admittance [4]. Sequence and superimposed components-based logic can be used for fault detection in the presence of Unified Power Flow Controller (UPFC) compensated lines [5], [6]. Impedance-based techniques and differential apparent power-based techniques are also developed to avoid the malfunctioning of relays in the presence of UPFC [7], [8], [9]. But these algorithms developed for compensated systems have considered only one type of device and its effects. They are not generalised algorithms but device-specific ones.

In fault location estimation, both mathematical techniques and computational intelligence techniques can be used for compensated and non-compensated transmission lines. The latter has the benefit that the fault detection or location estimation algorithm can be created without the necessity of a mathematical model of the system. In [10] and [11], a fuzzy system is utilised to identify the fault section and identify the defective phase using the current signals that have been wavelet-decomposed. The dc component and normalized peaks of the fundamental voltage and current are provided to the fuzzy-based fault locator and classifier in [12]. Reference [13] uses positive sequence impedance value fed to fuzzy inference scheme for fault location identification. Reference [14] employs wavelet transform to extract the features from transient fault current signals and a Generalised Neural Network (GNN) to identify the fault location. Artificial Neural Network (ANN)-based fault detector and locator with the magnitudes of voltage and current signals as input is presented in [15]. Wavelet Packet-ANN-based fault location technique utilizing the energy and entropy of current and voltage signals is described in [16]. The peak values of the post-fault fundamental components of voltages and currents are selected in [17] using extended Kalman filtering and Radial Basis Function Neural Network (RBFNN) is used for fault location and classification. Change in energy and standard deviation of fault current and voltage is calculated using HS transform and fed to an RBFNN to locate and classify the fault in [18]. Wavelet-based feature extraction and ANN-based fault location are presented in [19], [20], [21], [22], [23], [24], [25], and [26]. Reference [27] solves the fault location problem with the support vector regression method using the features extracted with the help of the stationary wavelet transform and determinant function feature. In [28], [29], [30], and [31] Support Vector Machine (SVM) based fault location methods are proposed. Energy coefficients of current signals [28], post-fault current signals and firing angle [29] or high-frequency contents of voltages and currents [30] can be used for the fault location estimation. ANFIS-based fault distance identification is presented in [32], [33], [34], [35], [36], [37], [38], and [39]. Three-line impedances are fed to an ANFIS-based fault locator to identify a single line to ground fault, in [32]. In [33] line impedance, measured from a single end, and the apparent impedance of SSSC, measured at terminals are utilized for fault location in an SSSC-compensated line. In [34] current signals from both ends are processed using wavelet transform and sixth-level Multiresolution Analysis (MRA) coefficients are fed to an ANFIS-based locator to estimate the fault location. Reference [35] uses wavelet transform and ANFIS to estimate fault location in parallel transmission lines. Reference [36] attempts fault location in transmission systems including underground cables using ANFIS. Reference [37] ANFIS-based fault location of series compensated lines using wavelet transform. Reference [38] employs FIS and ANFIS along with the wavelet MRA technic. Reference [39] fault location estimated using ANFIS with dc components frequency of voltage and current signals and phase angle between voltage and current.

On reviewing the literature on the fault location techniques in compensated lines, the following points are observed. In the voltage or current signal-based methods, different frequency components are required to be extracted which makes the computation complex. The impedance-based methods are simple compared to voltage or current-based methods. Variations of positive sequence impedance is utilised in most of the works for fault location estimation. For compensated lines, the variation of both positive and negative sequence impedance can be utilised to improve the accuracy of the estimation. Travelling wave-based methods are also used for faulty identification. But these methods require a high sampling rate. The computational intelligence methods are more suitable for compensated lines as they do not require the mathematical models of the compensating devices. With proper training, intelligent systems can accurately identify the faulty line and fault type or estimate the fault location.

This work attempts to develop an ANFIS-based fault locator that estimates the fault distance in a compensated line when it is identified as a faulty line. The ANFIS model has both numerical and linguistic knowledge. ANFIS-based fault location estimator does not require a mathematical model of the system, high sampling rates or the extraction of different frequency components for the estimation of fault distance. It requires comparatively a smaller number of data sets for the training process compared to other intelligent systems like ANN to give better results. It can be trained to produce accurate results, even without much expert knowledge. Conventional Fuzzy Inference System (FIS) needs expert knowledge to decide the membership function parameters to get the required results. ANFIS can construct a FIS whose membership function parameters are decided by the neural network part of the ANFIS using the training data set. It has

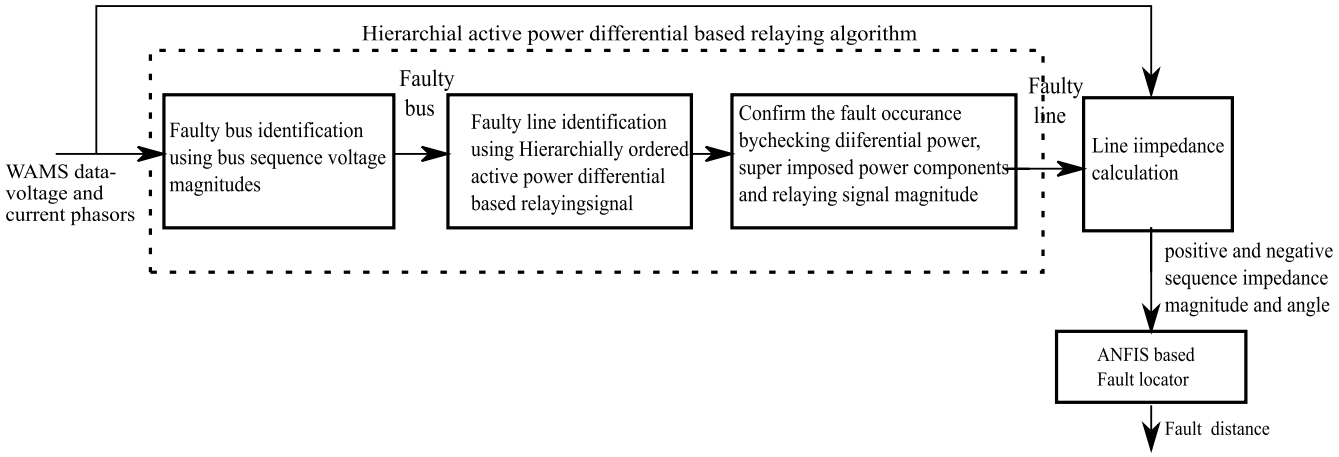

FIGURE 1. ANFIS based fault locator with hierarchical active power differential signal based faulty line identification algorithm using WAMS data.

the advantages of adaptation capability, nonlinear ability, and rapid learning capacity. A generalized backup protection scheme based on Wide Area Measurement System (WAMS) data that utilizes the power differential values of the lines is used for faulty line identification [40], [41]. The algorithm first identifies the buses near a fault with sequence components of bus voltages and then uses the hierarchial magnitudes of differential active power signals to identify the faulty line. This algorithm has the advantage that it reliably identifies the faulty line in a system containing series or shunt-compensated lines. The ANFIS-based fault locator calculates the positive and negative sequence impedance of a line with the voltage and current phasors received from phasor measurement units (PMUs) placed in different substations [42]. It estimates the fault location in a STATCOM or SSSC compensated line using the magnitude and phase angle of the sequence impedances thus calculated. To verify the performance of the proposed fault locator, a modified WSCC 9 bus system is built in the MATLAB/Simulink environment and different fault scenarios are created to get the data for training and testing. The real-world fault data (here the fundamental phasors of voltage and current) derived by the PMUs are noise free due to the inbuilt signal processing units. So the simulated fault data and the actual PMU data can be considered equivalent for the verification purpose. The key strategies employed in the fault location method presented in this work are

1. The algorithm for faulty line identification is a generalised backup protection algorithm that uses active power differential values to identify the faulty line. It can reliably identify the faulty line irrespective of the compensation device used in the system.

2. For the fault locator part, two separate ANFIS models are trained one for STATCOM and the other for SSSC so that a suitable model can be selected according to the actual device present in the line.

3. The ANFIS models are trained using 1450 training data sets generated with different combinations of fault types, fault resistances, fault distances and pre-fault loading.

4. The models are tested using 250 testing data sets which are generated with different combinations of fault conditions with values different from those in the training data set.

5. In all the test and training cases the maximum percentage error obtained is within 5 %.

The remaining sections of this paper are arranged as follows. Section II of this article provides the details of the proposed fault locator. Section III discusses the training details of the fault locator. The results obtained and the conclusion is presented in section IV and V.

II. PROPOSED ANFIS-BASED FAULT LOCATOR BASED ON WAMS DATA

The proposed ANFIS-based fault locator operates along with the hierarchial active power differential signal-based faulty line identification algorithm. The faulty line identification algorithm and the fault locator do not require the mathematical model of the compensating device or line. The algorithm identifies the faulty line with the help of sequence components of bus voltages and line currents and active power differential signals calculated utilizing the voltage and current phasor details obtained from WAMS data. After identifying the faulty line, the ANFIS-based fault locator estimates the fault distance using the positive and negative sequence impedance magnitudes and angles. the overall block diagram of the fault location estimation process is shown in Fig.1.

A. HIERARCHICAL ACTIVE POWER DIFFERENTIAL SIGNAL BASED ALGORITHM TO IDENTIFY THE FAULTY LINE

The faulty line identification algorithm collects the voltage and current phasors from all the substations in an area and identifies the faulty bus using the positive and negative sequence bus voltage magnitudes. When an unbalanced fault occurs in the system, the faulty bus is identified using the negative sequence bus voltage components, and when a balanced fault occurs, the faulty bus is identified using the positive sequence bus voltage components. Then it identifies the faulty line using the active power differential values

calculated for the lines connected to the faulty bus. The differential real power in a line and superimposed real power components of the line ends are used to confirm the faulty state of the line. The steps to be followed in the WAMS-based hierarchical active power differential algorithm are given below

Step 1: Collect the time-synchronized bus voltages and line currents from all the substations.

Step 2: Calculate the sequence components of all bus voltages.

Step 3: If the negative or zero sequence voltage component of any of the buses in the system is greater than the set threshold value, an unsymmetrical fault is suspected to have occurred in the system. Sort the buses in the descending order of the negative sequence bus voltage magnitude and identify the bus at the top of the sorted list as the faulty bus. ie,

$$|\vec{V}_{b2}| \leq K_2 V_N \tag{1}$$

or

$$|\vec{V}_{b0}| \leq K_0 V_N \tag{2}$$

where $\vec{V}_{b2}$ and $\vec{V}_{b0}$ are the negative and zero sequence components of b^{th} bus respectively in a B-bus system and V_N is the rated voltage magnitude of the bus, $K_2 V_N$ and $K_0 V_N$ are the thresholds whose values are selected such that all unbalanced faults in the system can be detected reliably.

Step 4: If the positive sequence voltage component of any of the buses in the system is less than the set threshold value, a symmetrical fault is suspected to have occurred in the system. Sort the buses in the ascending order of the positive sequence bus voltage magnitude and identify the bus at the top of the sorted list as the faulty bus.ie,

$$|\vec{V}_{b1}| \geq K_1 V_N \tag{3}$$

where $\vec{V}_{b1}$ is the positive sequence component of b^{th} bus, V_N is the rated voltage magnitude of the bus, and $K_1 V_N$ is the threshold whose value is selected such that all balanced faults in the system can be detected.

Step 5: Generate relaying signals $R = P_d/P_r$ for each line connected to the bus, where P_d and P_r are the difference and average of the active power at terminal 1 and terminal 2 of a line. ie,

$$R = \frac{P_d}{P_r} \tag{4}$$

$$P_d = |P_{terminal1} - P_{terminal2}| \tag{5}$$

$$P_r = \frac{(|P_{terminal1}| + |P_{terminal2}|)}{2} \tag{6}$$

For normal operation, these relaying signals will have negligible magnitudes.

Step 6: Identify the faulty line using the hierarchical order of the magnitudes of the relaying signal R calculated for the lines connected to the identified faulty bus and confirm it after checking the following conditions.

a. the magnitude of differential power, $|P_d|$, is greater than a set threshold value. This indicates an abnormal power drop in the line due to a fault.

b. the magnitude of superimposed power components, P_s, (difference in power calculated for consecutive cycles) in the line is greater than a set threshold value, P_{sT}. This indicates a sudden change in the system, like a fault.

$$P_s = P_{n^{th}cycle} - P_{(n1)^{th}cycle} \tag{7}$$

c. the value of the relaying signal falls in the internal fault region of the relay characteristics.

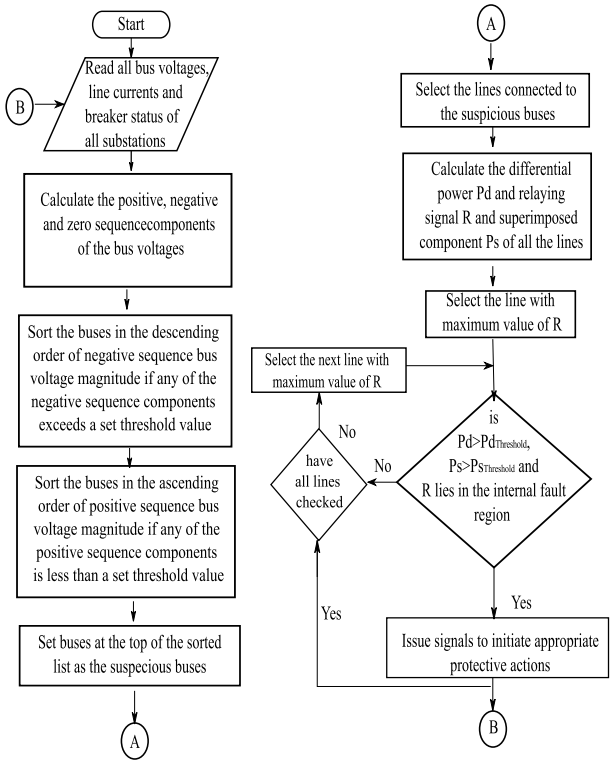

FIGURE 2. Flow chart of faulty line identification algorithm.

This algorithm is a generalised algorithm that effectively identifies the faulty line in both series and shunt-compensated systems. Fig. 2 shows the flow chart representation of the algorithm. Once the faulty line is identified, the proposed ANFIS-based fault locator identifies the fault distance.

In this study K_2 and K_0 are set as 0.1 pu, K_1 is set as 0.6 pu and P_{sT} as 0.05 pu

B. EFFECT OF STATCOM AND SSSC ON POWER FLOW IN FAULTY LINE

The presence of compensating device in line affects the power flow during fault. The variation in power flow for diffrent type of fault and fault distance is plotted for the compensated line 7-8. Fig. 3 shows the plots showing the effect of a STATCOM (shunt compensator) and a SSSC (series compensator). The effective impedance of the line is altered by the compensating action of the device. In both cases of

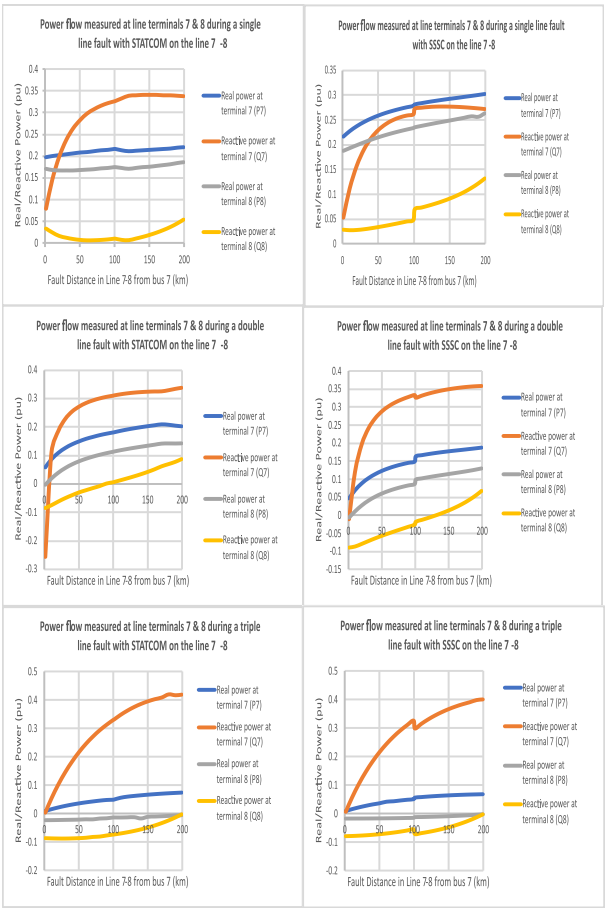

FIGURE 3. Power flow during differnt faults with different fault distances in a compensated line with STATTCOM and SSSC.

STATCOM and SSSC effective line impedance changes but as the SSSC is a series device its effect is more on the effective line impedance change. The impedance variation depends on the fault location, fault type and the location of the device. A properly trained intelligent fault locator based on the ANFIS can be developed that identifies the fault location when the efffective impedance variations are fed to it. In this paper the positive and negative impedance variations, with the compensating device at the midpoint of the line, are used for training the fault locator. Being an intelligent system ANFIS-based fault locator does not require the mathematical models of the devices. It learns the behavior of the compensator during fault from the training data presented to it. Here the compensating device is placed at the midpoint of the line ie, 100 km from terminal 7. It can be observed the power flow during fault conditions suddenly varies from the pattern followed when the fault distance is greater than 100km in the case of SSSC. When the SSSC is included in the fault loop, its effect on line impedance and hence on the power flow is more compared to that of STATCOM. This affects the ANFIS performance in learning the exact relationship between fault distance and impedance. So the accuracy of fault distance estimation is lower in the case of SSSC compared to that of STATCOM.

C. ANFIS-BASED FAULT LOCATOR

ANFIS combines the advantages of fuzzy inference methods and artificial neural networks (ANN). Its advantages include quick learning potential, nonlinearity, and adaptability. The learning process employs a hybrid or backpropagation method to reduce the difference between the observed and anticipated output.

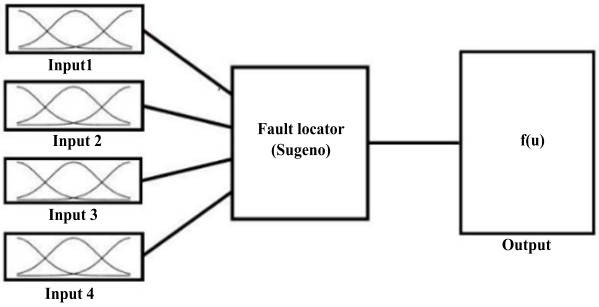

FIGURE 4. ANFIS Model for the fault locator.

ANFIS has the linguistic capabilities of a fuzzy system along with the learning and parallel computation capabilities of neural networks. ANFIS has a structure with 6 layers, viz, an input layer, fuzzification layer, rule layer, normalization layer, defuzzification layer, and summation layer. In the fuzzification layer, the input values are fuzzified using activation functions. The normalization layer calculates the normalized firing strength of the rules obtained from the rule layer, and the defuzzification layer calculates the weighted consequent value of a particular rule. The final ANFIS output is produced by the summation layer as the sum of all the defuzzification neurons' outputs. Any nonlinear and difficult problem can be solved with high accuracy by an ANFIS that has been properly developed and trained. The fault classification and fault location in compensated power systems can be done using ANFIS models. The proposed fault locator is an ANFIS structure of Sugeno type (Fig. 4). The fault locator can be used with the WAMS-based hierarchial active power differential algorithm for fault location estimation in a system with series or shunt-compensated line. The input of the fault locator are the magnitudes and angles of positive and negative sequence impedance of the line. The output of the fault locator is the fault location in km, measured from one terminal of the compensated line. Each input has five membership functions connected to it. The membership function employed is the gaussmf (Fig. 5). Data relating to various fault locations and fault resistances for all types of faults are used to train the ANFIS fault locator model. The training uses the hybrid learning approach.

The input and output data of the fault locator are shown in Table 1.

III. TRAINING DATA GENERATION FOR THE ANFIS-BASED FAULT LOCATOR

A modified WSCC 9-bus network is modelled in the MATLAB/Simulink environment by including the FACTS

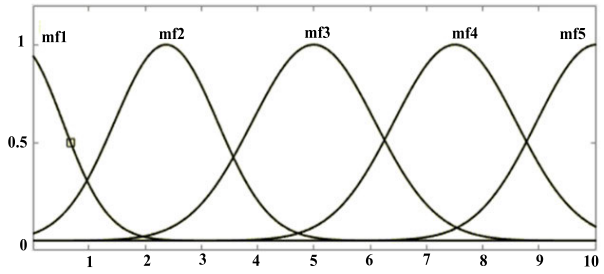

FIGURE 5. Input membership functions of type gaussmf.

TABLE 1. Fault locator input and output.

Input 1	Input 2	Input 3	Input 4	Output
Positive Sequence Impedance Magnitude	Positive Sequence Impedance Angle	Negative Sequence Impedance Magnitude	Negative Sequence Impedance Angle	Fault Location in km

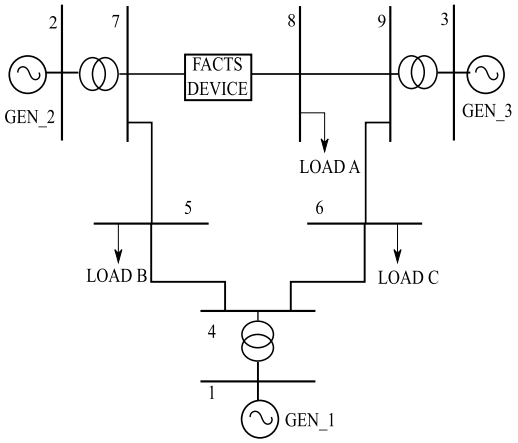

FIGURE 6. Modified WSCC 9 Bus system - single line diagram including FACTS device at the midpoint of line connected between bus 7 and bus 8.

TABLE 2. Various fault scenarios created for fault data generation.

Fault type	Fault resisatnce (Ω)	Fault distance (km)	Pre-fault loading (pu)
LG, LLG, LLLG, LL, LLL	Rf (Line-Line): 0.01, 0.1, 1 Rg (Line-ground) : 1, 10, 100	At every 10 km of line 7-8	0.2,0.9

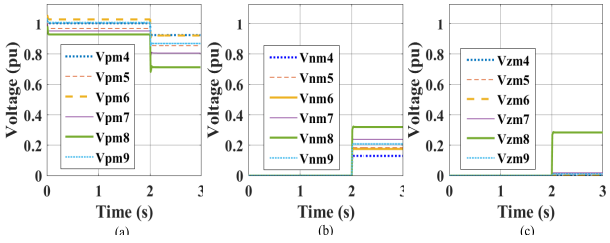

FIGURE 7. Variation of magnitudes of (a) positive sequence (b) negative sequence and (c) zero-sequence bus voltages for an LG fault at t=2s near Bus 8 in line 7-8.

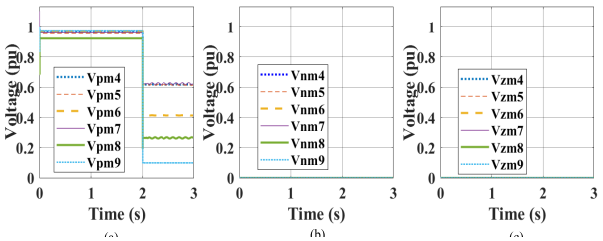

FIGURE 8. Variation of magnitudes of (a) positive sequence (b) negative sequence and (c) zero-sequence bus voltages for an LLL fault at t=2s near Bus 9 in line 8-9.

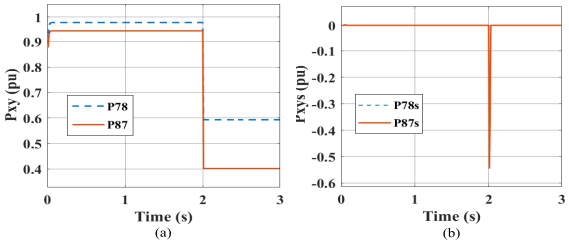

FIGURE 9. Variation of (a) P_{xy}, and (b) P_{xys} for an LG fault in Line 7-8 near bus 8.

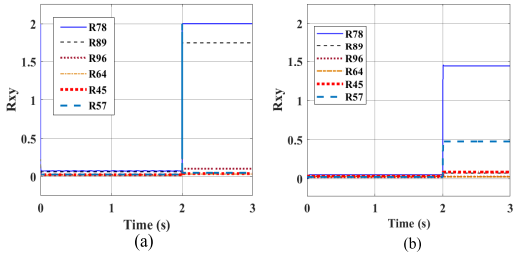

FIGURE 10. Variation of Rxy for various lines (R78, R89, R96, R64, R45, R57) for (a) an LLLG fault near bus 8 and (b) an LLG fault near bus 7 at t= 2s on line 7-8.

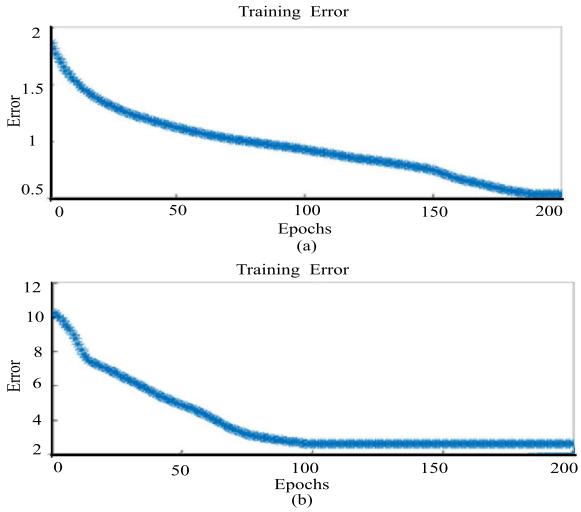

FIGURE 11. ANFIS training Error for (a) STATCOM compensated line (b) SSSC compensated line.

compensating device on line 7-8 (200 km long), as shown in Fig. 6. To generate the training data set, different fault scenarios are created in line 7-8 at every 10 km, with fault resistances of 1 Ω, 10 Ω, and 100 Ω. The pre-fault loadings

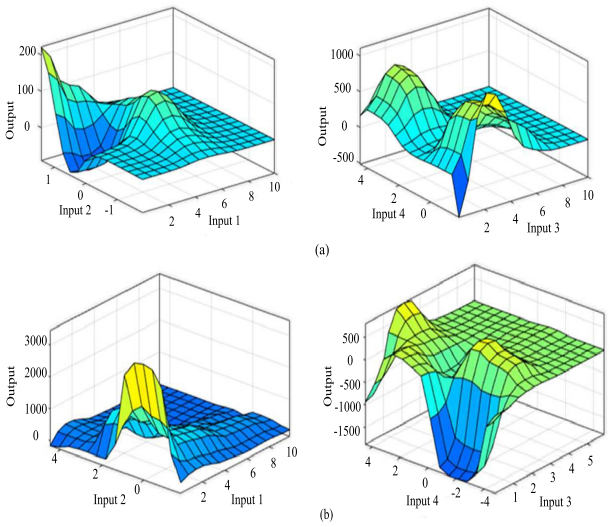

FIGURE 12. Surface view of input-output relation for ANFIS fault locator model for SSSC compensated line (a) output (fault location) vs positive sequence impedance magnitude (input1) and angle (input2) (b) output (fault location) vs negative sequence impedance magnitude (input3) and angle the(input4).

TABLE 3. Effect of fault location on the fault locator output and percentage error.

Fault type	Actual Fault location (km)	Fault on the section between bus 7 and STATCOM		Actual Fault location (km)	Fault on the section between STATCOM and bus 8	
		Fault locator	% Error		Fault locator	% Error
AG	10	6.43	1.78	115	115.20	0.10
BG	50	46.94	1.53	150	150.60	0.30
CG	90	89.14	0.43	180	181.10	0.05
ABG	8	6.94	0.53	192	192.06	0.03
BCG	40	40.20	0.1	145	145.10	0.05
ACG	25	24.76	0.12	167	167.30	0.15
AB	31	29.07	0.96	124	123.40	0.20
BC	76	74.94	0.53	188	188.30	0.15
AC	20	18.51	0.74	174	174.60	0.30
ABCG	60	59.72	0.14	105	104.55	0.22
ABC	95	95.53	0.26	135	135.2	0.10
Fault type	Actual Fault location (km)	Fault on the section between bus 7 and SSSC		Actual Fault location (km)	Fault on the section between SSSC and bus 8	
		Fault locator output	% Error		Fault locator output	% Error
AG	10	11.59	0.795	115	105.73	4.635
BG	50	50.41	0.205	150	145.6	2.2
CG	90	89.46	0.27	180	179.2	0.4
ABG	8	8.06	0.03	192	190.7	0.65
BCG	40	38.61	0.695	145	147.4	1.2
ACG	25	23.47	0.765	167	166.8	0.1
AB	31	30.09	0.455	124	124.3	0.15
BC	76	74.96	0.52	188	192.6	2.3
AC	20	18.28	0.86	174	175.5	0.75
ABCG	60	65.61	2.805	105	112.4	1.3
ABC	95	93.32	0.84	135	130.8	2.1

considered are 0.2 pu and 0.9 pu. 1450 training data sets are generated using the simulation of the network.

TABLE 4. Effect of fault resistance on the fault locator output and percentage error.

Fault type	Fault resistance (Ω)	Fault on the section between bus 7 and STATCOM			Fault on the section between STATCOM and bus 8		
		Actual Fault location (km)	Fault locator output (km)	% Error	Actual Fault location (km)	Fault locator output (km)	% Error
LG	5	50	47.90	1.05	150	151.2	0.06
	50	50	49.77	0.11	150	151.1	0.55
	90	50	49.54	0.23	150	150.3	0.15
LLG	5	50	50.02	0.01	150	149.9	0.05
	50	50	50.01	0.005	150	150.2	0.10
	90	50	49.97	0.015	150	150.3	0.15
LL	0.01	50	48.24	0.88	150	149.9	0.05
	0.1	50	48.46	0.77	150	149.9	0.05
	1	50	48.90	0.55	150	149.9	0.05
LLLG	5	50	49.82	0.09	150	150.5	0.25
	50	50	49.82	0.09	150	150.5	0.25
	90	50	49.82	0.09	150	150.5	0.25
LLL	0.01	50	53.06	1.53	150	152.8	1.4
	0.1	50	52.68	1.34	150	151.1	0.55
	1	50	49.83	0.08	150	150.5	0.25
Fault type	Fault resistance (Ω)	Fault on the section between bus 7 and SSSC			Fault on the section between SSSC and bus 8		
		Actual Fault location (km)	Fault locator output (km)	% Error	Actual Fault location (km)	Fault locator output (km)	% Error
LG	5	50	48.93	0.53	150	150.7	0.35
	50	50	50.46	0.23	150	153.2	1.6
	90	50	49.64	0.18	150	150.4	0.2
LLG	5	50	47.72	1.14	150	152.2	1.1
	50	50	45.1	2.45	150	155.2	2.6
	90	50	44.82	2.59	150	152.5	1.25
LL	0.01	50	49.01	0.49	150	150.9	0.45
	0.1	50	49.46	0.27	150	152.7	1.35
	1	50	48.38	0.81	150	151.3	0.65
LLLG	5	50	50.17	0.08	150	151.5	0.75
	50	50	50.46	0.23	150	148.0	1.00
	90	50	49.04	0.48	150	149.8	0.1
LLL	0.01	50	56.9	3.45	150	157.5	3.75
	0.1	50	54.36	2.18	150	154.5	2.25
	1	50	48.95	0.52	150	148.5	0.75

The fault conditions selected for data set generation are shown in Table 2

For both the SSSC and STATCOM cases, the magnitudes of the positive and negative sequence impedances and their angles are measured at the line end close to bus 7, and these values serve as the inputs to the fault locator.

IV. RESULTS

The faulty line identification algorithm is tested for different fault cases like LG, LLG, LLLG, LL and LLL in different lines by varying fault distances and line loading. In all cases the algorithm successfully identifies the faulty line.

The variation of bus voltages magnitudes during a balanced and unbalanced faults are shown in Fig. 7 and Fig. 8 respectively.

Variation of active power P_{xy} and superimposed power components P_{xys} at the line ends near bus 7 and bus 8 are shown in Fig. 9. The variation of relaying signals R_{xy} calculated for the different lines are shown for two different cases

TABLE 5. Effect of pre fault loading on the fault locator output and percentage error.

Fault type	Pre-fault loading (pu)	Fault on the section between bus 7 and STATCOM			Fault on the section between STATCOM and bus 8		
		Actual Fault location (km)	Fault locator output (km)	% Error	Actual Fault location (km)	Fault locator output (km)	% Error
LG	0.9	50	49.57	0.21	150	152.62	1.31
	0.5	50	48.11	0.94	150	151.51	0.75
	0.2	50	49.35	0.32	150	150.92	0.46
LLG	0.9	50	50.89	0.44	150	152.50	1.25
	0.5	50	51.22	0.61	150	151.19	0.59
	0.2	50	50.73	0.36	150	149.73	0.13
LL	0.9	50	49.91	0.04	150	151.95	0.95
	0.5	50	49.67	0.16	150	151.01	0.5
	0.2	50	49.23	0.38	150	149.59	0.2
LLL G	0.9	50	49.83	0.08	150	150.60	0.3
	0.5	50	49.73	0.13	150	150.48	0.24
	0.2	50	49.8	0.10	150	150.80	0.4
LLL	0.9	50	49.95	0.02	150	150.88	0.44
	0.5	50	50.2	0.10	150	150.5	0.25
	0.2	50	50.25	0.12	150	150.58	0.29
Fault type	Pre-fault loading (pu)	Fault on the section between bus 7 and SSSC			Fault on the section between SSSC and bus 8		
		Actual Fault location (km)	Fault locator output (km)	% Error	Actual Fault location (km)	Fault locator output (km)	% Error
LG	0.9	50	50.66	0.33	150	152.72	1.37
	0.5	50	47.51	1.25	150	151.53	0.77
	0.2	50	52.53	1.26	150	153.17	1.59
LLG	0.9	50	49.17	0.42	150	150.24	0.12
	0.5	50	51.36	0.68	150	150.89	0.45
	0.2	50	53.54	1.77	150	149.76	0.12
LL	0.9	50	49.38	0.31	150	148.42	0.79
	0.5	50	48.67	0.67	150	149.63	0.19
	0.2	50	50.32	0.16	150	149.18	0.41
LLL G	0.9	50	48.16	0.92	150	151.15	0.58
	0.5	50	47.85	1.08	150	153.09	1.55
	0.2	50	53.91	1.95	150	150.93	0.47
LLL	0.9	50	49.63	0.19	150	148.87	0.57
	0.5	50	48.55	0.73	150	150.54	0.27
	0.2	50	55.12	2.56	150	152.69	1.34

TABLE 6. Effect of fault inception angle on the fault locator output and percentage error.

Fault type	Fault inception angle (degree)	Fault on the section between bus 7 and STATCOM			Fault on the section between STATCOM and bus 8		
		Actual Fault location (km)	Fault locator output (km)	% Error	Actual Fault location (km)	Fault locator output (km)	% Error
LG	0	50	47.58	1.21	150	151.1	0.55
	90	50	47.58	1.21	150	151.1	0.55
	220	50	47.58	1.21	150	151.1	0.55
LLG	0	50	49.91	0.04	150	149.8	0.1
	90	50	49.91	0.04	150	149.8	0.1
	220	50	49.91	0.04	150	149.8	0.1
LL	0	50	48.5	0.75	150	149.9	0.05
	90	50	48.5	0.75	150	149.9	0.05
	220	50	48.5	0.75	150	140.9	0.05
LLL G	0	50	49.83	0.08	150	150.5	0.25
	90	50	49.83	0.08	150	150.5	0.25
	220	50	49.83	0.08	150	150.5	0.25
LLL	0	50	49.83	0.08	150	150.5	0.25
	90	50	49.83	0.08	150	150.5	0.25
	220	50	49.83	0.08	150	150.5	0.25
Fault type	Fault inception angle (degree)	Fault on the section between bus 7 and SSSC			Fault on the section between SSSC and bus 8		
		Actual Fault location (km)	Fault locator output (km)	% Error	Actual Fault location (km)	Fault locator output (km)	% Error
LG	0	50	49.89	0.05	150	152.20	1.1
	90	50	49.89	0.05	150	152.20	1.1
	220	50	49.89	0.05	150	152.20	1.1
LLG	0	50	49.61	0.19	150	150.42	0.21
	90	50	49.61	0.19	150	150.42	0.21
	220	50	49.61	0.19	150	150.42	0.21
LL	0	50	48.82	0.59	150	149.18	0.41
	90	50	48.82	0.59	150	149.18	0.41
	220	50	48.82	0.59	150	149.18	0.41
LLL G	0	50	47.95	1.02	150	152.76	1.38
	90	50	47.95	1.02	150	152.76	1.38
	220	50	47.95	1.02	150	152.76	1.38
LLL	0	50	49.04	0.48	150	149.13	0.44
	90	50	49.04	0.48	150	149.13	0.44
	220	50	49.04	0.48	150	149.13	0.44

in Fig. 10. The magnitude of relaing signal of the faulty line is highest in both cases.

The fault locator model is trained by utilizing input-output data sets gathered during the simulation of various fault scenarios. For the training of the ANFIS fault locator, the hybrid learning approach is chosen. The membership function selected is gaussmf. The STATCOM fault locator and SSSC fault locator parts are trained separately to learn the input-output relation. 625 rules for the STATCOM part and 1296 rules for the SSSC part are created by the ANFIS model itself during the learning process. Training error is converged to 0.54 in 194 epochs for the STATCOM part and to 2.65 in 100 epochs for the SSSC part (Fig. 11). The average error obtained for the former is 0.62 and for the latter is 2.93. The surface views of input-output relationships formed by the fault locator are shown in Fig. 12.

Testing of the fault locator is done using input-output data sets generated by varying one of the parameters like fault distance, fault resistance, pre-fault loading or fault inception angle, keeping other parameters constant. 250 data sets are generated for the testing purpose which were not used for the training purpose.

The performance of the fault locator is consolidated in Table 3 to 6. Table 3 is the results obtained by varying the fault distance keeping the fault type, fault resistance, pre-fault loading, and fault inception angle random. It is found from Table 3 that the results are more accurate for the STATCOM module of the fault locator and the error is comparatively higher for the SSSC module. A worst-case difference of around 8 km is obtained in some cases. For long lines, the error is negligible considering the total length of the line. The percentage error is found as follows

$$\%\ Error = \frac{|L_{f,actual} - L_{f,output}|}{L_{line}} x100 \tag{8}$$

where $L_{f,ctual}$ is the actual fault location, $L_{f,output}$ is the fault locator output and L_{line} is the line length.

The variation of error is shown in Fig. 13. For practical purposes the maximum percentage error of less than 5% obtained is acceptable.

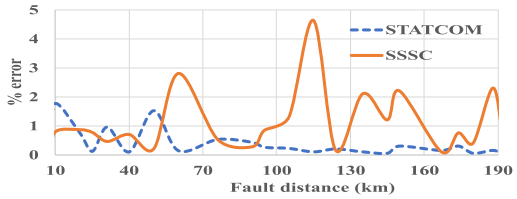

FIGURE 13. Effect of distance on the fault locator performance.

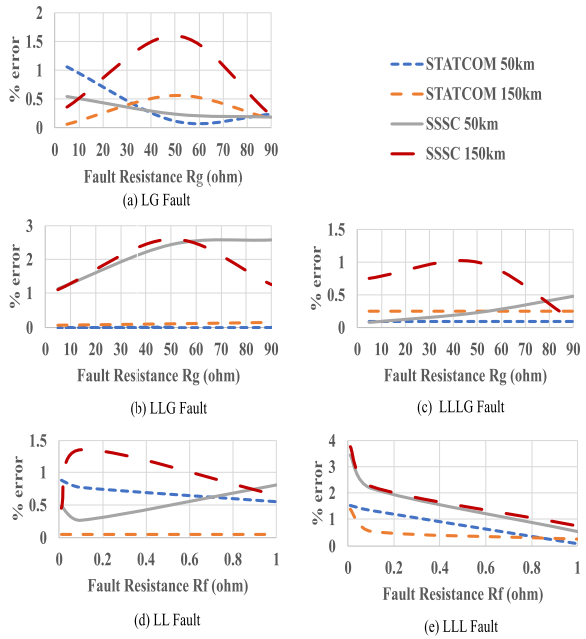

FIGURE 14. Effect of fault resistance on the fault locator performance.

Table 4 shows the variation of the error with fault resistance for different types of faults created at a distance of 50 km and 150 km from bus 7. Here fault inception angle and pre-fault loading were kept constant. Fig. 14 is the graphical representation of the result. The percentage error is below 5% in all cases. Variation of the error with pre-fault loading is consolidated in Table 5. Fault inception angle and fault resistance are kept constant in this case. The Maximum percentage error obtained is 2.5%. Table 6 shows the variation in the error with fault inception angle while fault resistance and pre-fault loading is kept constant. The fault inception angle has no effect on the error and the error is below 1.5%. Fig. 15 and Fig. 16 depict the results shown in Table 5 and Table 6 respectively.

Comparing the proposed fault location method with model-free techniques available in the literature the following points are highlighted- [12], [13], [16], and [19] use fuzzy-based or ANN-based fault location estimation for uncompensated lines. Input quantities in [12] and [13] are positive sequence impedance and fundamental frequency components of voltage and current respectively with reported accuracy of 95% and 92%. References [16] and [19]

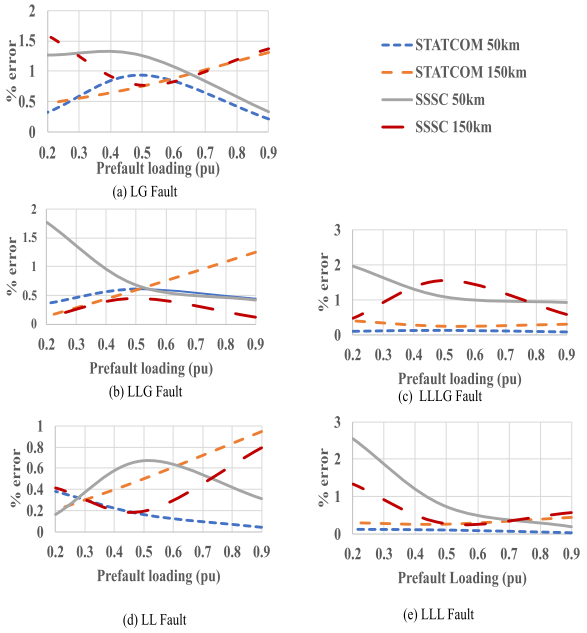

FIGURE 15. Effect of prefault loading on the fault locator performance.

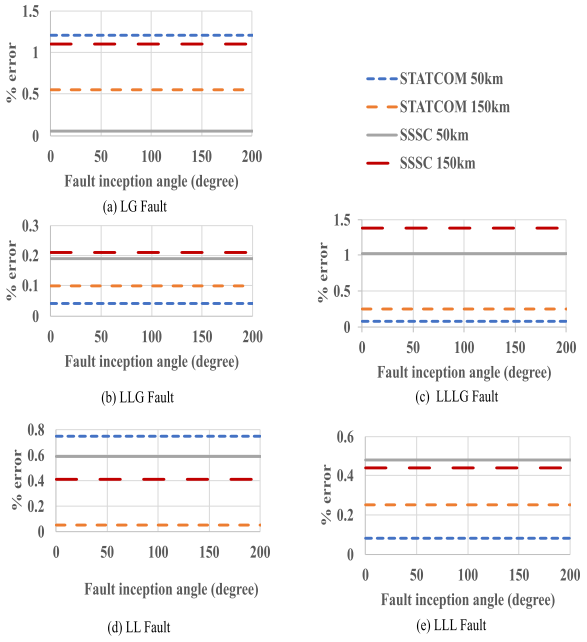

FIGURE 16. Effect of fault inception angle on the fault locator performance.

utilises the statistical features extracted from current and voltage signals using wavelet decomposition techniques. Reference [16] has 90% accuracy and [19] has 95% accuracy. References [43], [44], [45], [46], [47], [48], [49], [50], and [51] are fault estimation techniques for FACTS compensated lines. They use frequency transform techniques to extract the required details and an intelligent tool to estimate the fault location in shunt (STATCOM), series (TCSC/SSSC) and UPFC compensated lines (Table 7). All these techniques

TABLE 7. Comparison with the proposed method and other methods.

Technique	FACTS Device	Double or single end	Fault resistance considered	Accuracy
Sequence impedance details-ANFIS (Proposed method)	STATCOM, SSSC	Single end	Up to 100	>98% for STATCOM >95% for SSSC
DWT- Game Theory [43]	STATCOM	Single end	Up to 50	>99%
DFT-ANN [44]	STATCOM	Single end	Up to 100	>98%
WT- ANN [45]	STATCOM	Double end	Up to 15	>98%
S-Transform- Logistic Model Tree (ST-LMT) [46]	TCSC	Single end	Up to 100	>97%
WT-ANN, WPT ANN [47]	TCSC	Single end	Up to 50	>99%
DWT [48]	SSSC	Single end	Up to 50	>98%
FDOST-SVM [49]	UPFC	Single end	Up to 100	>97%
Sparse S-transform (SST) [50]	UPFC	Single end	Up to 200	>94%
WT -ANN [51]	UPFC	Double end	Up to 100	>98%

have more than 98% accuracy. But they need frequency details extraction from voltage and current signals. The main advantage of the proposed technique is that it needs only fundamental frequency components of voltage and current signals which are obtained from the PMUs placed in substations. So, it requires less computational requirements. Also, ANFIS can be trained with a smaller number of datasets to produce sufficiently accurate results compared to other intelligent tools. The proposed fault location technique is suitable for both shunt and series compensated lines. It gives more than 98% accuracy in STATCOM-compensated lines and more than 95% accuracy in SSSC-compensated lines.

V. CONCLUSION

An ANFIS - based fault locator acting in conjunction with the hierarchial active power differential-based faulty line identification algorithm utilizing the WAMS data is investigated in this paper. The faulty line identification algorithm successfully identifies the faulty line using the sequence voltage phasors and active power differential-based relaying signals of the suspected lines. As the algorithm uses the active power differential signals, it is effective in identifying the faulty line in both shunt and series compensated systems. The fault locator uses the magnitude and angle of the positive and negative sequence impedances. During training, ANFIS networks develop the rules for estimating the fault location using their learning capabilities. The Simulation results show that fault locators based on ANFIS are suitable for locating faults in compensated lines. It is capable of accurately estimating the location of the fault with 5% of tolerance. The advantage of this method is that the fault location estimation requires only the positive and negative sequence impedance details calculated using the fundamental components, it does not require the details of other frequency components, and being an intelligent system-based method it can system can be trained to suit both compensated and uncompensated lines.

REFERENCES

[1] P. K. Nayak, A. K. Pradhan, and P. Bajpai, "Wide-area measurement-based backup protection for power network with series compensation," *IEEE Trans. Power Del.*, vol. 29, no. 4, pp. 1970–1977, Aug. 2014.

[2] M. K. Jena, S. R. Samantaray, and B. K. Panigrahi, "A new wide-area backup protection scheme for series-compensated transmission system," *IEEE Syst. J.*, vol. 11, no. 3, pp. 1877–1887, Sep. 2017.

[3] S. K. Mishra, L. N. Tripathy, and S. C. Swain, "A DWT based differential relaying scheme of SVC compensated line," in *Proc. Int. Conf. Innov. Mech. Ind. Appl. (ICIMIA)*, Feb. 2017, pp. 295–301.

[4] P. Khadke, N. Patne, A. Singh, and G. Shinde, "Pilot relaying scheme based on differential admittance concept for FSC-compensated EHV transmission line," *Iranian J. Sci. Technol., Trans. Electr. Eng.*, vol. 44, no. 2, pp. 949–961, Jun. 2020.

[5] S. Biswas and P. K. Nayak, "Superimposed component-based protection scheme for UPFC compensated transmission lines," in *Proc. 20th Nat. Power Syst. Conf. (NPSC)*, Dec. 2018, pp. 1–6.

[6] M. Khederzadeh, "Application of synchrophasors to adaptive protection of transmission lines compensated by UPFC," in *Proc. 10th IET Int. Conf. Develop. Power Syst. Protection (DPSP). Manag. Change*, Apr. 2010, pp. 1–5.

[7] B. Mallikarjuna, A. Saggurthi, M. J. B. Reddy, and D. K. Mohanta, "PMU based distance protection methodology to avert malfunction due to FACTS controllers," in *Proc. 20th Nat. Power Syst. Conf. (NPSC)*, Dec. 2018, pp. 1–6.

[8] B. Kumar and A. Yadav, "Backup protection scheme for transmission line compensated with UPFC during high impedance faults and dynamic situations," *IET Sci., Meas. Technol.*, vol. 11, no. 6, pp. 703–712, Sep. 2017.

[9] M. Abasi, A. Saffarian, M. Joorabian, and S. Ghodratollah Seifossadat, "Fault classification and fault area detection in GUPFC-compensated double-circuit transmission lines based on the analysis of active and reactive powers measured by PMUs," *Measurement*, vol. 169, Feb. 2021, Art. no. 108499.

[10] A. K. Pradhan, A. Routray, S. Pati, and D. K. Pradhan, "Wavelet fuzzy combined approach for fault classification of a series-compensated transmission line," *IEEE Trans. Power Del.*, vol. 19, no. 4, pp. 1612–1618, Oct. 2004.

[11] O. A. S. Youssef, "Combined fuzzy-logic wavelet-based fault classification technique for power system relaying," *IEEE Trans. Power Del.*, vol. 19, no. 2, pp. 582–589, Apr. 2004.

[12] P. K. Dash, A. K. Pradhan, and G. Panda, "A novel fuzzy neural network based distance relaying scheme," *IEEE Trans. Power Del.*, vol. 15, no. 3, pp. 902–907, Jul. 2000.

[13] A. Yadav and A. Swetapadma, "Enhancing the performance of transmission line directional relaying, fault classification and fault location schemes using fuzzy inference system," *IET Gener., Transmiss. Distrib.*, vol. 9, no. 6, pp. 580–591, Apr. 2015.

[14] M. Jamil, A. Kalam, A. Q. Ansari, and M. Rizwan, "Generalized neural network and wavelet transform based approach for fault location estimation of a transmission line," *Appl. Soft Comput.*, vol. 19, pp. 322–332, Jun. 2014.

[15] T. Bouthiba, "Fault location in EHV transmission lines using artificial neural networks," *Int. J. Appl. Math. Comput. Sci.*, vol. 14, no. 1, pp. 69–78, 2004.

[16] S. Ekici, S. Yildirim, and M. Poyraz, "Energy and entropy-based feature extraction for locating fault on transmission lines by using neural network and wavelet packet decomposition," *Expert Syst. Appl.*, vol. 34, no. 4, pp. 2937–2944, May 2008.

[17] A. K. Pradhan, P. K. Dash, and G. Panda, "A fast and accurate distance relaying scheme using an efficient radial basis function neural network," *Electr. Power Syst. Res.*, vol. 60, no. 1, pp. 1–8, Nov. 2001.

[18] S. R. Samantaray, P. K. Dash, and G. Panda, "Fault classification and location using HS-transform and radial basis function neural network," *Electr. Power Syst. Res.*, vol. 76, nos. 9–10, pp. 897–905, Jun. 2006.

[19] S. Sahoo, P. Ray, B. K. Panigrahi, and N. Senroy, "A computational intelligence approach for fault location in transmission lines," in *Proc. Joint Int. Conf. Power Electron., Drives Energy Syst. Power India*, Dec. 2010, pp. 1–6.

[20] A. Jain, A. S. Thoke, and R. N. Patel, "Double circuit transmission line fault distance location using artificial neural network," in *Proc. World Congr. Nature Biologically Inspired Comput. (NaBIC)*, Dec. 2009, pp. 13–18.
[21] A. Swetapadma and A. Yadav, "All shunt fault location including cross-country and evolving faults in transmission lines without fault type classification," *Electr. Power Syst. Res.*, vol. 123, pp. 1–12, Jun. 2015.
[22] A. Dasgupta, S. Nath, and A. Das, "Transmission line fault classification and location using wavelet entropy and neural network," *Electr. Power Compon. Syst.*, vol. 40, no. 15, pp. 1676–1689, Oct. 2012.
[23] A. R. Adly, R. A. El Sehiemy, A. Y. Abdelaziz, and N. M. A. Ayad, "Critical aspects on wavelet transforms based fault identification procedures in HV transmission line," *IET Gener., Transmiss. Distrib.*, vol. 10, no. 2, pp. 508–517, Feb. 2016.
[24] A. Yadav and A. Swetapadma, "A single ended directional fault section identifier and fault locator for double circuit transmission lines using combined wavelet and ANN approach," *Int. J. Electr. Power Energy Syst.*, vol. 69, pp. 27–33, Jul. 2015.
[25] S. R. Samantaray, P. K. Dash, and G. Panda, "Distance relaying for transmission line using support vector machine and radial basis function neural network," *Int. J. Electr. Power Energy Syst.*, vol. 29, no. 7, pp. 551–556, Sep. 2007.
[26] S. Ekici, "Support vector machines for classification and locating faults on transmission lines," *Appl. Soft Comput.*, vol. 12, no. 6, pp. 1650–1658, Jun. 2012.
[27] A. A. Yusuff, A. A. Jimoh, and J. L. Munda, "Fault location in transmission lines based on stationary wavelet transform, determinant function feature and support vector regression," *Electr. Power Syst. Res.*, vol. 110, pp. 73–83, May 2014.
[28] M. J. B. Reddy, P. Gopakumar, and D. K. Mohanta, "A novel transmission line protection using DOST and SVM," *Eng. Sci. Technol., Int. J.*, vol. 19, no. 2, pp. 1027–1039, Jun. 2016.
[29] P. K. Dash, S. R. Samantaray, and G. Panda, "Fault classification and section identification of an advanced series-compensated transmission line using support vector machine," *IEEE Trans. Power Del.*, vol. 22, no. 1, pp. 67–73, Jan. 2007.
[30] R. Salat and S. Osowski, "Accurate fault location in the power transmission line using support vector machine approach," *IEEE Trans. Power Syst.*, vol. 19, no. 2, pp. 979–986, May 2004.
[31] Z. Moravej, M. Khederzadeh, and M. Pazoki, "New combined method for fault detection, classification, and location in series-compensated transmission line," *Electr. Power Compon. Syst.*, vol. 40, no. 9, pp. 1050–1071, Jun. 2012.
[32] M. Paul and S. Debnath, "ANFIS based single line to ground fault location estimation for transmission lines," in *Proc. Michael Faraday IET Int. Summit (MFIIS)*, vol. 2020, Oct. 2020, pp. 69–74.
[33] E. Mohagheghi, A. Bagherian, W. A. Ashiru, and A. Esmaeilian, "A new fault location method based on adaptive neuro fuzzy in presence of SSSC on transmission line," in *Proc. 11th Int. Conf. Environ. Electr. Eng.*, May 2012, pp. 108–111.
[34] E. S. M. T. Eldin, "Fault location for a series compensated transmission line based on wavelet transform and an adaptive neuro-fuzzy inference system," in *Proc. Electr. Power Quality Supply Rel. Conf.*, Jun. 2010, pp. 229–236.
[35] R. Meyur, D. Pal, N. A. Sundaravaradan, P. Rajaraman, K. V. V. S. Srinivas, M. J. B. Reddy, and D. K. Mohanta, "A wavelet-adaptive network based fuzzy inference system for location of faults in parallel transmission lines," in *Proc. IEEE Int. Conf. Power Electron., Drives Energy Syst. (PEDES)*, Dec. 2016, pp. 1–6.
[36] C. K. Jung, K. H. Kim, J. B. Lee, and B. Klöckl, "Wavelet and neuro-fuzzy based fault location for combined transmission systems," *Int. J. Electr. Power Energy Syst.*, vol. 29, no. 6, pp. 445–454, Jul. 2007.
[37] H. Eristi, "Fault diagnosis system for series compensated transmission line based on wavelet transform and adaptive neuro-fuzzy inference system," *Measurement*, vol. 46, no. 1, pp. 393–401, Jan. 2013.
[38] M. J. Reddy and D. K. Mohanta, "A Wavelet-neuro-fuzzy combined approach for digital relaying of transmission line faults," *Electr. Power Compon. Syst.*, vol. 35, no. 12, pp. 1385–1407, Sep. 2007.
[39] J. Sadeh and H. Afradi, "A new and accurate fault location algorithm for combined transmission lines using adaptive network-based fuzzy inference system," *Electr. Power Syst. Res.*, vol. 79, no. 11, pp. 1538–1545, Nov. 2009.
[40] F. Namdari, S. Jamali, and P. Crossley, "Power differential based wide area protection," *Iranian J. Electr. Electron. Eng.*, vol. 1, no. 3, pp. 53–66, 2005.
[41] S. Venugopal, P. Asok, and S. R. Arya, "WAMS-based hierarchical active power differential signal algorithm for backup protection of a FACTS compensated transmission network," *Adv. Electr. Electron. Eng.*, vol. 20, no. 4, pp. 390–404, Feb. 2023.
[42] V. Sreelekha and A. Prince, "ANFIS based fault locator for STATCOM compensated lines," in *Proc. 2nd Int. Conf. Next Gener. Intell. Syst. (ICNGIS)*, Jul. 2022, pp. 1–4.
[43] M Khalili, F. Namdari, and E. Rokrok, "A fault location and detection technique for STATCOM compensated transmission lines using game theory," *IET Gener., Transmiss. Distrib.*, vol. 15, no. 11, pp. 1688–1701, 2021.
[44] S. Sowmya Nagam, E. Koley, and S. Ghosh, "Artificial neural network based fault locator for three phase transmission line with STATCOM," in *Proc. IEEE Int. Conf. Comput. Intell. Comput. Res. (ICCIC)*, Dec. 2017, pp. 1–4.
[45] B. Rathore, O. P. Mahela, B. Khan, H. H. Alhelou, and P. Siano, "Wavelet-alienation-neural-based protection scheme for STATCOM compensated transmission line," *IEEE Trans. Ind. Informat.*, vol. 17, no. 4, pp. 2557–2565, Apr. 2021.
[46] Z. Moravej, M. Pazoki, and A. A. Abdoos, "A new approach for fault classification and section detection in compensated transmission line with TCSC," *Eur. Trans. Electr. Power*, vol. 21, no. 1, pp. 997–1014, Jan. 2011.
[47] P. Ray, B. K. Panigrahi, and N. Senroy, "Hybrid methodology for fault distance estimation in series compensated transmission line," *IET Gener., Transmiss. Distrib.*, vol. 7, no. 5, pp. 431–439, May 2013.
[48] E. Reyes-Archundia, J. L. Guardado, E. L. Moreno-Goytia, J. A. Gutierrez-Gnecchi, and F. Martinez-Cardenas, "Fault detection and localization in transmission lines with a static synchronous series compensator," *Adv. Electr. Comput. Eng.*, vol. 15, no. 3, pp. 17–22, 2015.
[49] Z. Moravej, M. Pazoki, and M. Khederzadeh, "New pattern-recognition method for fault analysis in transmission line with UPFC," *IEEE Trans. Power Del.*, vol. 30, no. 3, pp. 1231–1242, Jun. 2015.
[50] L. Tripathy, S. R. Samantaray, and P. K. Dash, "Sparse S-transform for location of faults on transmission lines operating with unified power flow controller," *IET Gener., Transmiss. Distrib.*, vol. 9, no. 15, pp. 2108–2116, Nov. 2015.
[51] B. Rathore, O. Prakash Mahela, B. Khan, and S. Padmanaban, "Protection scheme using wavelet-alienation-neural technique for UPFC compensated transmission line," *IEEE Access*, vol. 9, pp. 13737–13753, 2021.

V. SREELEKHA received the bachelor's degree in electrical and electronics engineering from the Rajiv Gandhi Institute of Technology, Kottayam, India, in 2001, and the master's degree from the College of Engineering, Trivandrum, India, in 2003. She is currently pursuing the Ph.D. degree with APJ Abdul Kalam Technological University, Kerala.

In 2011, she joined the Department of Electrical Engineering, Rajiv Gandhi Institute of Technology, Kottayam, as an Assistant Professor. Her research interests include power systems, wide-area measurements, smart grids, and microgrids.

A. PRINCE (Senior Member, IEEE) received the bachelor's degree in electrical and electronics engineering from the Thangal Kunju Musaliar College of Engineering, Kollam, India, in 1996, and the master's and Ph.D. degrees in electrical engineering from the Indian Institute of Technology, Delhi, India, in 2005 and 2012, respectively.

He is currently a Professor in electrical engineering with the Rajiv Gandhi Institute of Technology, Kottayam, Kerala, India. His research interests include power systems, renewable energy systems, wide area measurements, electric vehicles and signal processing applications in power systems, power electronics applications in power systems, and artificial intelligence applications in power systems.

Dr. Prince has contributed as a Reviewer of IEEE TRANSACTIONS ON POWER SYSTEMS and IEEE TRANSACTIONS ON INDUSTRIAL ELECTRONICS.